This article has been accepted for publication in a future issue of this journal, but has not been fully edited. Content may change prior to final publication. Citation information: DOI 10.1109/TPWRS.2019.2892014, IEEE Transactions on Power Systems

A Complex-Valued Three-Phase Load Flow for Radial Networks: High-Performance and Low-Voltage Solution Capability

Jonattan E. Sarmiento, Cristian A. Alvez, B. de Nadai N., *Student Members, IEEE*, A.C. Zambroni de Souza, Edgar M. Carreno, *Senior Members, IEEE*, and Paulo F. Ribeiro, *Fellow, IEEE*.

***Abstract*—Load flow methods for distribution networks such as Backward Forward Sweep (BFS) have a good computational performance and can find solutions with accuracy. However, some studies may demand the determination of low voltage solutions, and this poses a problem for these methods since they cannot find these solutions due to convergence issues. This paper presents a load flow method based on a novel complex-valued formulation developed for distribution networks, which works well on radial topologies by using an incidence matrix to avoid complicated series element models, allow high-performance and low-voltage solution capability. The formulation is solved by Newton's method via Wirtinger's calculus. To prove the low-voltage solution capability, both sides of QV curves, i.e., unstable and stable regions were traced on balanced and unbalanced networks. Performance tests in the IEEE test feeders show that the runtime is less than or equal to the runtime of the BFS method. Furthermore, the line R/X ratio and the number of controlled voltage node or volt-var functions do not affect the computational performance, yielding advantages over the classic Newton and BFS methods.**

***Index Terms*—Complex-valued formulation, distribution networks, load flow, low-voltage solutions, Newton's method, QV curves, transformer connections, volt-var function, Wirtinger's calculus.**

I. Nomenclature

Variables

I_0	Current of the reference node
I_N	Vector of nodal currents (except reference node)
I_Y, I_Δ and I_{sh}	Vectors of the star, delta and shunt currents
I_B	Vector of branches' flow currents
ΔV_B	Vector of branches' voltage drops
V_N	Vector of nodes' phase voltages
V_Δ	Vector of nodes' line voltages
f	Vector mismatch function of the voltage drops
S_G, S_{LY}, and $S_{L\Delta}$	Vector of generation power, and star and delta loads.
S_{LZY}, S_{LIY} and S_{LPY}	Vectors of ZIP star load components (constant impedance, current, and power)
$S_{LZ\Delta}$, $S_{LI\Delta}$ and $S_{LP\Delta}$	Vectors of ZIP delta load components (constant impedance, current, and power)
f_{PV} and f_{VV}	Vector mismatch functions of the PV and VV nodes
V_{PV} and V_{1PV}	Vectors of nodal and positive-sequence voltages of the PV nodes
V_{VV} and V_{1VV}	Vectors of nodal and positive-sequence voltages of the VV nodes
S_{PV} and S_{VV}	Vectors of complex powers of the PV and VV nodes
f_{GV} and S_{GV}	Vector function of mismatches, and complex powers of the generation nodes (PV and VV)
T	Matrix of branch's turns ratio

Parameters

L	Incidence matrix
L_0 and L_c	Submatrices of L
N	Number of nodes (except reference node)
$[Z_B]$	Block diagonal matrix of the branch's impedances
$[Y_{sh}]$	Block diagonal matrix of the nodes' shunt admittances
V_R	Voltage constant of the reference node
$[YD]$	Block diagonal matrix for the phase to line voltage conversion
S_{L0Y} and $S_{L0\Delta}$	Vectors of the total star and delta loads at nominal voltage.
Z_P, Z_Q, I_P, I_Q, P_P, and P_Q	Vectors of ZIP coefficients
N_{PV} and N_{VV}	Number of PV and VV nodes
$[A_{PV}]$ and $[A_{VV}]$	Block diagonal matrices for the phase to positive-sequence voltage conversion of the PV and VV nodes
P_{PV} and P_{VV}	Vectors of specified active powers of the PV and VV nodes

Operators

$\odot$	Element-wise product between two vectors
$1/(\cdot)$	Element-wise reciprocal of a vector
$(\cdot)^*$	Conjugate of a vector or matrix
$(\cdot)^T$	Transpose of a vector or matrix
$(\cdot)^H$	Conjugate transpose of a vector or matrix

This work was supported in part by CAPES (Brazilian research agency)

This article has been accepted for publication in a future issue of this journal, but has not been fully edited. Content may change prior to final publication. Citation information: DOI 10.1109/TPWRS.2019.2892014, IEEE Transactions on Power Systems

II. Introduction

THE QV and PV curves provide important information about voltage stability of a system. In transmission systems, these curves are traced by Continuation Power Flow (CPF) techniques [1], [2]. These techniques use Newton's method to solve the real-valued load flow formulation, and its Jacobian matrix helps to predict the curves' points and to detect bifurcation and unstable points.

Voltage stability analyses for distribution networks were not necessary for the past, nevertheless, over the last decade, these networks are evolving from static overplanned networks to dynamic active systems which will require operation planning similar to transmission systems in some aspects. The main reason for this transformation is the increased penetration of distributed generators (DG) [3].

In this new reality, the existent tools to analyze distribution systems no longer support the information needs for the new decision-making process to operate this networks. One such area in need of new tools is voltage stability analyses. This is the reason why the feasibility of CPF in distribution networks should be revised; what it implies to have effective and efficient load flow methods available.

One of the load flow methods most widely used in distribution networks is the Backward Forward Sweep (BFS) [4], developed by taking advantage of the radial topology, resulting in an efficient tool. However, the lack of a Jacobian matrix makes it impractical to use into CPF techniques. Furthermore, the BFS method can't find points of the left side of QV curves or the low side of PV curves, due to convergence issues on low voltage solutions [5].

Traditional Newton's method for real-valued formulation in polar form, used in transmission systems, have been developed for balanced systems, and its computational performance is improved by decoupling techniques, however, these techniques are not suitable for radial unbalanced distribution networks with high line R/X ratios [6]. A load flow method that has a Jacobian matrix and computational performance similar to BFS would be more desirable to plot QV and PV curves.

Some load flow methods with direct [7]–[9] or improved BFS [10]–[12] approaches have been proposed in the literature. However, their iterative processes are similar to BFS, and low voltage solutions could be infeasible. In [13], a non-iterative method is presented, but the accuracy decreases in low voltage solutions. Furthermore, all aforementioned methods don't employ a Jacobian matrix.

References [14]–[17] present methods and analyses for load flow formulations using Wirtinger's calculus. This framework straightforwardly obtains a Jacobian matrix of a complex-valued function to be used in Newton's method. In this way, the authors solve the complex-valued formulation without the need to split it into two real-valued formulations. Even though the proposals are shown as robust, these references don't explain details of unbalanced three-phase element models, and elements such as ideal or shifting transformers are complicated to include in the system's admittance matrix (matrix used in their formulations). To deal with this last issue, approaches with an incidence matrix [7]–[9] could be used and to model series elements through impedances instead of admittances.

In summary, voltage stability studies are becoming more important in the increasingly active distribution networks, therefore, a three-phase load flow method for these networks with the following features is necessary:

- Find any type of load flow solution (high and low voltage);
- Being able to work with radial topologies;
- Allow to easily model any three-phase element of a distribution network: unbalanced star and delta loads, ZIP load model, three-phase lines with mutual impedances, On-Load Tap Changer (OLTC), DG operating in controlled voltage mode or with volt-var functions, among others;
- Provide high computational performance;
- Have a Jacobian matrix.

This paper proposes a load flow method, which presents all of these characteristics. It is based on a novel complex-valued formulation developed specifically for unbalanced radial networks through an incidence matrix. The formulation is solved, in the same way as [16] and [17], by Newton's method using Wirtinger's calculus, preserving the powerful convergence property of Newton's method [14].

The text is organized as follows: In section III, the load flow formulation is presented. Section IV introduces the models of common elements in distribution networks. Section V presents the iterative solution technique. Section VI shows how to trace QV curves using the proposed load flow method. Section VII perform load flow performance tests and explores the low-voltage solution capability by tracing QV curves. Finally, the main conclusions are exposed.

III. Load Flow Formulation

The formulation proposed in this paper, called Radial Complex-valued Formulation (RCF), compares branch voltage drops calculated by two modes, one calculated from injected nodal currents and another from node voltages. The load flow problem is considered solved when both voltage drops match. All magnitudes are expressed in per-unit (p.u.).

A. *Incidence Matrix*

The voltage drop calculations use matrices based on the incidence matrix L, which is explained below.

In (1), the matrix shows the relationships between the injected nodal and branch flow currents of the system depicted in Fig. 1. The node 0 is the reference node and there is a transformer between nodes 3 and 4.

$$\begin{bmatrix} I_0 \\ I_1 \\ I_2 \\ I_3 \\ I_4 \\ I_5 \end{bmatrix} = \begin{bmatrix} \mathrm{I} & & & & & \\ -\mathrm{I} & \mathrm{I} & \mathrm{I} & & & \\ & -\mathrm{I} & & & & \\ & & -\mathrm{I} & T^H & & \\ & & & -\mathrm{I} & \mathrm{I} & \\ & & & & & -\mathrm{I} \end{bmatrix} \begin{bmatrix} I_{B1} \\ I_{B2} \\ I_{B3} \\ I_{B4} \\ I_{B5} \end{bmatrix} \quad (1)$$

The value I_i is the three-phase nodal current of node i, and I_{Bj} is the branch flow current of branch j. Each column of L is associated with a branch and each row with a node. The following steps form the matrix.

This article has been accepted for publication in a future issue of this journal, but has not been fully edited. Content may change prior to final publication. Citation information: DOI 10.1109/TPWRS.2019.2892014, IEEE Transactions on Power Systems

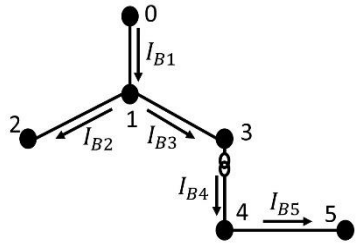

Fig. 1. Radial network

For each branch (column):
- Set −I in the ending node.
- Set T^H in the sending node.

where I is the identity matrix of size 3x3, and T is the matrix of transformer ratio. $(\cdot)^H$ denotes conjugate transpose. For lines without transformer $T = \mathrm{I}$, and Appendix D shows T for several transformer connections. Thus, once formed L for any system with the aforementioned steps; equation (2) defines the relationship between the injected nodal I and branch flow I_B currents according to Kirchhoff's current law.

$$I = L\, I_B \tag{2}$$

Also, the sum of branch power losses of a system is equal to the sum of injected nodal powers, expressed in (3). ΔV_B and V are the branch voltage drops and node voltages, respectively.

Replacing (2) in (3) yields (4). This equation shows the relationships between ΔV_B and V according to Kirchhoff's voltage law.

$$I_B{}^H \Delta V_B = I^H V \tag{3}$$

$$\Delta V_B = L^H\, V \tag{4}$$

It is essential to observe that L provides the relationship between currents; and its conjugate transpose L^H provides the relationship between voltages, which is very useful.

B. *Branch voltage drops calculated from injected nodal currents*

Equation (2) is written in (5), where I_0 and I_N are injected currents by the reference node and others N nodes, respectively. L_0 is made taking three rows of L related to the reference node. Thus, for a radial network with $(N+1)$ nodes and N branches, the matrix L_C is square and (6) can be written.

$$\begin{bmatrix} I_0 \\ I_N \end{bmatrix} = \begin{bmatrix} L_0 \\ L_C \end{bmatrix} I_B \tag{5}$$

$$I_B = L_C{}^{-1} I_N \tag{6}$$

For a branch j, the voltage drop is $\Delta V_{Bj} = Z_{Bj}\, I_{Bj}$, being Z_{Bj} the branch's impedance matrix. By placing all ΔV_{Bj} in a vector (7) is obtained, which provides ΔV_B using as variable I_N. Where $[Z_B]$ is a block diagonal matrix formed by the impedance matrices of all branches.

$$\Delta V_B = [Z_B]\, L_C{}^{-1}\, I_N \tag{7}$$

C. *Branch voltage drops calculated from node voltages*

Equation (4) is expanded as shown in (8), where V_0 and V_N are voltages of the reference node and the other N nodes, respectively. Finally, (9) provides ΔV_B calculated by means of V_N. Being $V_R = L_0{}^H\, V_0$ a voltage constant related to the reference node.

$$\Delta V_B = \begin{bmatrix} L_0 \\ L_C \end{bmatrix}^H \begin{bmatrix} V_0 \\ V_N \end{bmatrix} \tag{8}$$

$$\Delta V_B = V_R + L_C{}^H\, V_N \tag{9}$$

D. *Load flow problem formulation*

The goal is to match equations (7) and (9). For this purpose, (10) defines a vector function f, and the load flow problem is solved when V_N leads f to become zero.

$$f = V_R + L_C{}^H\, V_N - [Z_B]\, L_C{}^{-1}\, I_N \tag{10}$$

The vector of nodal currents I_N depends on voltage, load and generator powers, and shunt admittances of each node:

$$\begin{aligned} I_N &= I_Y + [YD]^T I_\Delta + I_{sh} \\ I_Y &= (S_G^* - S_{LY}^*) \odot \frac{1}{V_N^*} \\ I_\Delta &= -\left(S_{L\Delta}^* \odot \frac{1}{V_\Delta^*} \right) \\ I_{sh} &= -[Y_{sh}] V_N \\ V_\Delta &= [YD]\, V_N \end{aligned} \tag{11}$$

where $[Y_{sh}]$ and $[YD]$ are block diagonal matrices. $[Y_{sh}]$ is formed by shunt admittances of all nodes, and the phase to line voltage conversion matrix $[YD]$ by N matrices yd (12). The vectors S_G, S_{LY}, and $S_{L\Delta}$ are the concatenation of three-phase values of generation power, star and delta load of all nodes, respectively, and V_Δ contains line voltages.

$$yd = \begin{bmatrix} 1 & -1 & 0 \\ 0 & 1 & -1 \\ -1 & 0 & 1 \end{bmatrix} \tag{12}$$

Note that f is computed by V_N and I_N through constant matrices, yielding simplicity in calculations.

IV. Models

This section presents the models of the elements usually present in a distribution network.

A. *ZIP load model with star and delta connections*

The vectors S_{LY} and $S_{L\Delta}$ depend on V_N and V_Δ, as shown in (13) and (14), respectively. Vectors S_{L0Y} and $S_{L0\Delta}$ are the star and delta loads of all nodes at nominal voltage, and Z_P, Z_Q, I_P, I_Q, P_P, and P_Q are the ZIP coefficients.

$$\begin{aligned} S_{LY} &= S_{LZY} \odot V_N \odot V_N^* + S_{LIY} \odot [V_N \odot V_N^*]^{1/2} + S_{LPY} \\ S_{LZY} &= \mathrm{Re}(S_{L0Y}) \odot Z_P + j\ \mathrm{Im}(S_{L0Y}) \odot Z_Q \\ S_{LIY} &= \mathrm{Re}(S_{L0Y}) \odot I_P + j\ \mathrm{Im}(S_{L0Y}) \odot I_Q \\ S_{LPY} &= \mathrm{Re}(S_{L0Y}) \odot P_P + j\ \mathrm{Im}(S_{L0Y}) \odot P_Q \end{aligned} \tag{13}$$

$$\begin{aligned} S_{L\Delta} &= S_{LZY} \odot V_\Delta \odot V_\Delta^* + S_{LIY} \odot [V_\Delta \odot V_\Delta^*]^{1/2} + S_{LP\Delta} \\ S_{LZ\Delta} &= \left(\mathrm{Re}(S_{L0\Delta}) \odot Z_P + j\ \mathrm{Im}(S_{L0\Delta}) \odot Z_Q\right)/3 \\ S_{LI\Delta} &= \left(\mathrm{Re}(S_{L0\Delta}) \odot I_P + j\ \mathrm{Im}(S_{L0\Delta}) \odot I_Q\right)/\sqrt{3} \\ S_{LP\Delta} &= \mathrm{Re}(S_{L0\Delta}) \odot P_P + j\ \mathrm{Im}(S_{L0\Delta}) \odot P_Q \end{aligned} \tag{14}$$

B. *Distributed generators*

Notice that ZIP load models enable one to emulate a generator. Such emulation is achieved by modeling the load as

This article has been accepted for publication in a future issue of this journal, but has not been fully edited. Content may change prior to final publication. Citation information: DOI 10.1109/TPWRS.2019.2892014, IEEE Transactions on Power Systems

a negative power. Hence, generators that operate with a constant current or some desired mode of operation addressed by suitable ZIP parameters can be modeled through the load model presented above. Also, three generator models are developed below.

1) Constant power (PQ node)

Each generator modeled as PQ node operates keeping constant the generation power. Hence, its power must be merely specified in the vector S_G.

2) Controlled voltage (PV node)

Each generator operates controlling its positive sequence voltage and keeping active power constant. The power injection is balanced.

For each PV node i, a function $f_{PV,i}$ is defined as:

$$\begin{aligned} f_{PV,i} &= \left(v_{1,i}\, v_{1,i}^{*} - {v_{sp,i}}^{2}\right) + j\,\left(\frac{s_{PV,i}+s_{PV,i}^{*}}{2} - p_{sp,i}\right) \\ v_{1,i} &= a v_i \\ a &= 1/3\,[1 \quad e^{j2\pi/3} \quad e^{-j2\pi/3}] \end{aligned} \tag{15}$$

The value of $f_{PV,i}$ must be zero. The real part of $f_{PV,i}$ is the condition that makes matching the positive sequence voltage magnitude $|v_{1,i}|$ and specified voltage $v_{sp,i}$, and the imaginary part is the condition that makes matching $\mathrm{Re}(s_{PV,i})$ and specified active power $p_{sp,i}$. Being $s_{PV,i}$ the generation power, and v_i the three-phase node voltage.

All $f_{PV,i}$ of N_{PV} PV nodes can be expressed compactly by a vector function:

$$\begin{aligned} f_{PV} &= \left(V_{1PV} \odot V_{1PV}^{*} - {V_{sp}}^{2}\right) + j\,\left(\frac{S_{PV}+S_{PV}^{*}}{2} - P_{PV}\right) \\ V_{1PV} &= [A_{PV}]\, V_{PV} \end{aligned} \tag{16}$$

where the block diagonal matrix $[A_{PV}]$ is formed by N_{PV} matrices a. The vector V_{PV} is the v_i concatenation of all PV nodes.

3) Volt-Var functions (VV node)

The active power remains constant, and reactive power depends linearly on the magnitude of positive sequence voltage using a piecewise linear function. The volt-var function is defined through K points $(v_k\,, Q_k)$ that determine $(K-1)$ intervals [18]:

$$\begin{aligned} Q &= Q_k + n_k(|v_1| - v_k) \\ n_k &= \frac{Q_{k+1} - Q_k}{v_{k+1} - v_k} \end{aligned} \tag{17}$$

The value k must be chosen according to current voltage and the intervals.

For each VV node i, a function $f_{VV,i}$ is defined as:

$$\begin{aligned} f_{VV,i} &= Q_{k,i} + n_{k,i}\left[\left(v_{1,i} v_{1,i}^{*}\right)^{\frac{1}{2}} - v_{k,i}\right] + j\left(s_{VV,i} - p_{sp,i}\right) \\ v_{1,i} &= a v_i \end{aligned} \tag{18}$$

The value of $f_{VV,i}$ must be zero. The real part of $f_{VV,i}$ is the condition that makes matching the reactive power given by the volt-var function, and $\mathrm{Im}(s_{VV,i})$, and the imaginary part is the condition that makes matching $\mathrm{Re}(s_{VV,i})$ and specified active power $p_{sp,i}$, being $s_{VV,i}$ the generation power.

All $f_{VV,i}$ of N_{VV} VV nodes can be expressed compactly by a vector function:

$$\begin{aligned} f_{VV} &= Q_k + N_k \odot \left[\left(V_{1VV} \odot V_{1VV}^{*}\right)^{\frac{1}{2}} - V_k\right] + j\,(S_{VV} - P_{VV}) \\ V_{1VV} &= [A_{VV}]\, V_{VV} \end{aligned} \tag{19}$$

where the block diagonal matrix $[A_{VV}]$ is formed by N_{VV} matrices a. The vector V_{VV} is the v_i concatenation of all VV nodes.

C. *On-Load Tap Changer*

The tap positions of an OLTC assume discrete values. Hence, the model employed does not use continuous values and is similar to the methodology already presented in [4], explained below for convenience.

Every time the load flow is solved, the tap positions of OLTCs (turns ratio matrix T) must be updated, returning to the load flow again, until the tap positions do not change.

Typically, the regulator is used to increase or decrease the voltage up to 10%, and the range of tap positions is from -16 to 16. Therefore, T is calculated with:

$$T = \mathrm{I} + 0.1/16 \times \mathrm{diag}(tap_a \quad tap_b \quad tap_c) \tag{20}$$

The tap positions must be updated with the following steps:

- Check if secondary voltages v_s are within the lower and upper voltage bounds.
- If v_s is out of bounds, set v_s to the limit, and calculate the continuous tap value to finally round it to the nearest allowed position.

V. The Newton's Method and Wirtinger's Calculus Applied to Load Flow Problem

The load flow problem is solved when f and f_{GV} are zero:

$$\begin{bmatrix} f_{(V_N, S_{GV})} \\ f_{GV(V_N, S_{GV})} \end{bmatrix} = 0 \tag{21}$$

where $f_{GV} = [f_{PV} \quad f_{VV}]^T$ and $S_{GV} = [S_{PV} \quad S_{VV}]^T$.

Since the problem is nonlinear, an iterative method must be used. The Newton's method can be applied to complex-valued problems using the Wirtinger's calculus [19].

A. *Wirtinger's calculus*

Given a vector function $h_{(z)}$, containing z and z^* as independent variables, it's possible to write the Taylor's expansion of $h_{(z,z^*)}$ and its conjugate $h_{(z,z^*)}^{*}$ [20], [21]. Hence, Newton's method can be applied to the vector function $F_{(z,z^*)}$:

$$\begin{aligned} F_{(z,z^*)} &= \begin{bmatrix} h_{(z,z^*)} \\ h_{(z,z^*)}^{*} \end{bmatrix} \\ J &= \begin{bmatrix} j_A & j_B \\ j_C & j_D \end{bmatrix} = \begin{bmatrix} \dfrac{\partial h_{(z,z^*)}}{\partial z} & \dfrac{\partial h_{(z,z^*)}}{\partial z^*} \\ j_B^{*} & j_A^{*} \end{bmatrix} \end{aligned} \tag{22}$$

where J is the Jacobian matrix of $F_{(z,z^*)}$. The equalities $j_C = j_B^{*}$ and $j_D = j_A^{*}$ [21] reduces the number of calculations.

B. *Reformulation of the load flow problem*

In order to apply Newton's method to (21), a new vector function is defined $F_{(V_N, S_{GV}, V_N^{*}, S_{GV}^{*})}$, and the load flow problem is solved when:

This article has been accepted for publication in a future issue of this journal, but has not been fully edited. Content may change prior to final publication. Citation information: DOI 10.1109/TPWRS.2019.2892014, IEEE Transactions on Power Systems

$$F_{(V_N, S_{GV}, V_N^*, S_{GV}^*)} = \begin{bmatrix} f_{(V_N, S_{GV}, V_N^*, S_{GV}^*)} \\ f_{GV(V_N, S_{GV}, V_N^*, S_{GV}^*)} \\ f^*_{(V_N, S_{GV}, V_N^*, S_{GV}^*)} \\ f^*_{GV(V_N, S_{GV}, V_N^*, S_{GV}^*)} \end{bmatrix} = 0 \quad (23)$$

Although the sizes of the vector function and the vector of variables are doubled (remember that V_N^* and S_{GV}^* are considered as independent variables of V_N and S_{GV} in Wirtinger's calculus), in this way $F_{(V_N, S_{GV}, V_N^*, S_{GV}^*)}$ is an analytic function. This fact allows calculating the Jacobian matrix without the need to split the formulation into two real-valued formulations.

C. *Jacobian and inverse Jacobian matrices*

The Jacobian matrix of $F_{(V_N, S_{GV}, V_N^*, S_{GV}^*)}$ is formed by

$$J = \begin{bmatrix} j_A & j_B \\ j_B^* & j_A^* \end{bmatrix}$$

$$j_A = \begin{bmatrix} \frac{\partial f_{(V_N, S_{GV}, V_N^*, S_{GV}^*)}}{\partial V_N} & \frac{\partial f_{(V_N, S_{GV}, V_N^*, S_{GV}^*)}}{\partial S_{GV}} \\ \frac{\partial f_{GV(V_N, S_{GV}, V_N^*, S_{GV}^*)}}{\partial V_N} & \frac{\partial f_{GV(V_N, S_{GV}, V_N^*, S_{GV}^*)}}{\partial S_{GV}} \end{bmatrix} \quad (24)$$

$$j_B = \begin{bmatrix} \frac{\partial f_{(V_N, S_{GV}, V_N^*, S_{GV}^*)}}{\partial V_N^*} & \frac{\partial f_{(V_N, S_{GV}, V_N^*, S_{GV}^*)}}{\partial S_{GV}^*} \\ \frac{\partial f_{GV(V_N, S_{GV}, V_N^*, S_{GV}^*)}}{\partial V_N^*} & \frac{\partial f_{GV(V_N, S_{GV}, V_N^*, S_{GV}^*)}}{\partial S_{GV}^*} \end{bmatrix}$$

And the inverse Jacobian matrix J^{-1} by

$$J^{-1} = \begin{bmatrix} \Gamma_A & \Gamma_B \\ \Gamma_B^* & \Gamma_A^* \end{bmatrix}$$

$$\begin{aligned} \Gamma_A &= [j_A - M\, j_B^*]^{-1} \\ \Gamma_B &= -\Gamma_A M \\ M &= j_B\, j_A^{*-1} \end{aligned} \quad (25)$$

Each component of j_A and j_B are explained in Appendix A and J^{-1} in Appendix B.

D. *Updating variables*

In order to decrease the number of calculations, only $\Delta z = [\Delta V_N \quad \Delta S_{GV}]^T$ will be calculated, since $[\Delta V_N^* \quad \Delta S_{GV}^*]^T$ is the conjugate of Δz. Equation (26) is obtained from (25), see Appendix C for details.

$$\begin{aligned} \Delta z &= \Gamma_A(M h^* - h) \\ h &= \begin{bmatrix} f \\ f_{GV} \end{bmatrix} \end{aligned} \quad (26)$$

E. *Load flow algorithm*

Fig. 2 depicts the flowchart of the load flow algorithm. The operator $|\cdot|$ is the Euclidean norm and ε a predefined mismatch tolerance.

VI. Tracing QV curves

The QV curve is traced by setting a PV node with different specified voltages V_{sp}. It is convenient to use a predicted step Δz with respect to Δp, being $z = [V_N \quad S_{PV}]^T$ and $p = {V_{sp}}^2$.

From CPF technique, it is known that

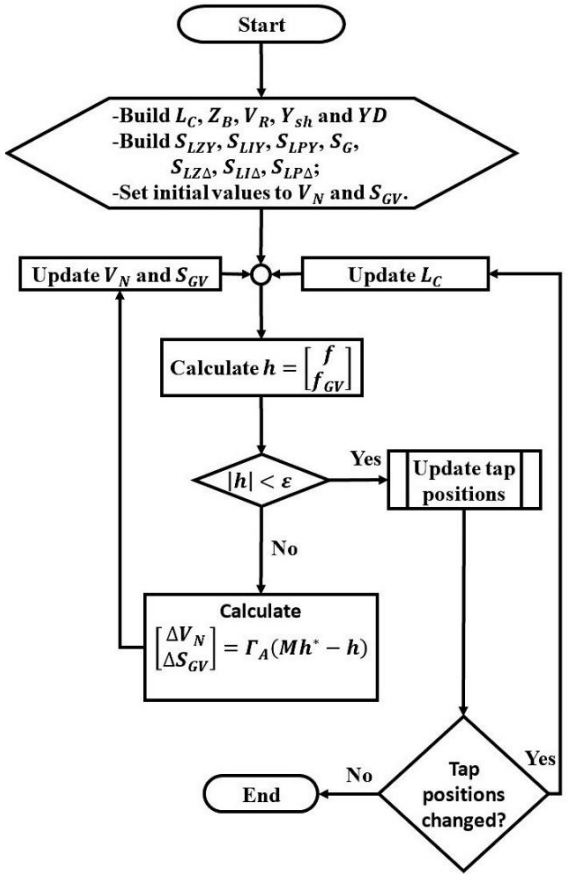

Fig. 2. Load flow algorithm

$$\Delta z = -J^{-1}\, \frac{\partial F}{\partial p}\, \Delta p$$

where $\frac{\partial F}{\partial p}$ is obtained by differentiating $F_{(V_N, S_{PV}, V_N^*, S_{PV}^*)}$, which gives a vector filled with zeros except in two positions that have the value -1. These positions are those corresponding to the specified voltage of the PV node in f_{PV}:

$$\frac{\partial F}{\partial p} = \begin{bmatrix} \frac{\partial f}{\partial p} & \frac{\partial f_{PV}}{\partial p} & \frac{\partial f^*}{\partial p} & \frac{\partial f_{PV}^*}{\partial p} \end{bmatrix}^T = \begin{bmatrix} 0 \\ -1 \\ 0 \\ -1 \end{bmatrix}$$

VII. Results and Discussions

This section shows the robustness of the load flow method proposed (RCF, named homonymous to formulation). First, the computational performance of RCF is tested. Then, the ability to deal with low voltage solutions is explored by tracing QV curves.

A. *Performance tests*

The algorithms were implemented in Matlab® and the processor used is Intel® Core™ i7-3770 @ 3.40GHz. The performance tests are carried out in IEEE 13, 34 and 123 node test feeders [22]. All tests start with flat node voltages; the power base is 3 MVA and the mismatch tolerance is 10^{-8} p.u.

Table I shows the errors with respect to results given by the IEEE's official summaries; the maximum error was 52.5×10^{-5} p.u. A computational performance comparison is carried out between RCF and one of the most efficient methods for radial networks, the BFS method [4]. Results show that the

This article has been accepted for publication in a future issue of this journal, but has not been fully edited. Content may change prior to final publication. Citation information: DOI 10.1109/TPWRS.2019.2892014, IEEE Transactions on Power Systems

TABLE I
Base case of IEEE test feeders

System	Error (10^{-5} p.u.)			Runtime (ms)			No. of iterations		
	Ph-1	Ph-2	Ph-3	RCF	BFS	Ratio	RCF	BFS	Ratio
IEEE-13	4.3	5.7	11.4	2	42	21.00	3	9	3.00
IEEE-34	13.8	16.5	14.1	8	73	9.13	3	12	4.00
IEEE-123	**52.5**	20.5	19.8	125	117	0.94	2	8	4.00
Average						**10.35**			**3.67**

TABLE II
Convergence vs. R/X ratio

R/X	Without DG		1 PV node		2 PV nodes	
	No. of iterations	Runtime (ms)	No. of iterations	Runtime (ms)	No. of iterations	Runtime (ms)
67.5724	3	8.2	-	-	-	-
6.9723	3	8.3	-	-	-	-
3.8859	3	8.3	5	15.0	6	16.5
3.5673	3	8.3	4	11.0	5	14.5
1.7949	**3**	**8.0**	**3**	**8.1**	**4**	**11.0**
0.5937	3	7.9	3	8.2	4	11.0
0.0003	3	8.2	3	8.1	4	11.2

average ratio of runtimes is 10.35 and the average rate of the number of iterations 3.67. The RCF demonstrates much higher runtime performance with 13 and 34 nodes (~15 times faster); nevertheless, it shows a small decrease in performance with 123 nodes (0.94). The latter may be due to increase in the size of the vector function and its Jacobian matrix.

Several combinations of average line R/X ratios and generator models were tested in the unbalanced IEEE-34 nodes feeder to assess the RCF convergence. Average R/X value of the positive sequence impedances is used as R/X index; this value for the base case is 1.7949. Table II shows the number of iterations and the runtime by changing the R/X ratio on-diagonal elements of the three-phase impedance matrices, keeping their magnitudes constant. Note that without DG, R/X ratio does not affect the number of iterations, which is an advantage over the decoupled Newton's method for real-valued formulation. However, with one and two PV nodes, the number of iterations increases as R/X ratio increases, but it is not due to the RCF performance, this is because the system is close to voltage collapse (note that this is not a feasible solution analysis, just an explanation of the increases in the iterations of the method). The capability to control the voltage injecting reactive power decreases when R/X increases, which causes the system to collapse due to the large flow of reactive power through the lines.

Finally, DGs modeled as PV and VV nodes, injecting zero active power, were inserted on IEEE-34 nodes feeder. These models could represent modern devices such as smart inverters. The voltages of PV nodes are set in 1.05 p.u. Table III displays the volt-var function configuration points.

The results in Table IV show that the load flow is solved in 3 or 4 iterations for several numerical combinations of PV and VV nodes. Therefore, RCF performance is practically not sensitive to the number of generators, which is an advantage over some methods; for instance, BFS method is sensitive to VV nodes and a technique should be used to improve their convergence as shown in [18].

TABLE III
Volt-var function configuration

Point	1	2	3	4
V	0.00	0.95	1.05	2.00
Q	2.00	2.00	-2.00	-2.00

TABLE IV
No. of iterations for PV vs. VV nodes

PV \ VV	0	1	2	3	4	5
0	3	3	3	3	4	4
1	3	3	4	4	4	4
2	4	4	4	4	4	4
3	4	4	4	4	4	4
4	4	4	4	4	4	4
5	4	4	4	4	4	4

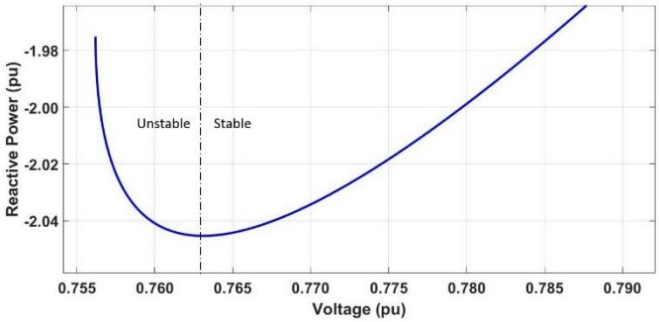

(a) Node 675 (IEEE-13 node test feeder)

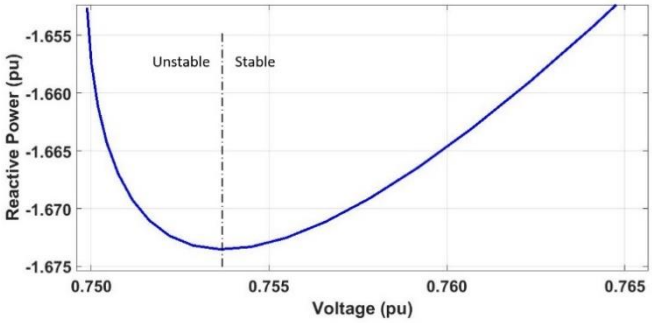

(b) Node 300 (IEEE-123 node test feeder)

Fig. 3. QV curves in unbalanced networks

B. *QV curves*

Firstly, the QV curves (including the left side) are traced through RCF on unbalanced IEEE 13 and 123 node test feeders. In the second part, the IEEE-34 test is considered as balanced and two QV curves are traced in the same node in order to be compared; one traced by RCF and another by a well-known CPF technique for transmission (CPF-T) [1].

1) Unbalanced three-phase networks

Fig. 3(a) and (b) show QV curves of nodes 675 and 300, respectively. Both sides of the curves (unstable and stable) are plotted while that BFS would find points of the right side only.

2) Balanced network

The IEEE-34 node test feeder is balanced modeling each load as a constant power of value equal at its three-phase average and modeling each line through its positive sequence impedance only.

This article has been accepted for publication in a future issue of this journal, but has not been fully edited. Content may change prior to final publication. Citation information: DOI 10.1109/TPWRS.2019.2892014, IEEE Transactions on Power Systems

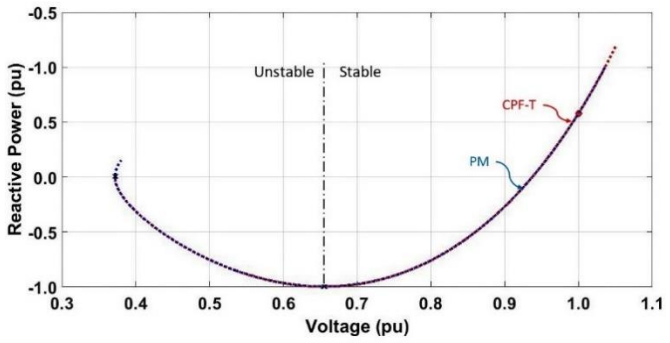

Fig. 4. QV curve of node 828 (IEEE-34 node test feeder balanced)

Fig. 4 shows the QV curve of node 828 traced via RCF and CPF-T. Both curves are identical. The runtime by RCF is just 6 s while CPF-T uses 36 s.

VIII. Conclusions

This paper has presented a load flow method based on a novel complex-valued formulation developed for unbalanced radial networks.

The formulation takes advantage of radial topologies, being solved the load flow in a few milliseconds. In tests performed on the IEEE test feeders with less than 100 nodes, the runtime was less than BFS runtime, but with more than 100 nodes, the computational performances become similar perhaps due to an increase in the size of matrices. The method could be improved in this regard.

The line R/X ratio does not affect the computational performance, an advantage over the decoupled Newton's method for real-valued formulation. The number of PV or VV nodes at most increased one iteration the process, an advantage over the BFS method.

The method can find low voltage solutions, which is an essential feature in voltage stability analysis. This fact provides an important advantage over other methods developed for distribution networks such as BFS.

Appendix A

A. *Differentiation of* $f_{(V_N, S_{GV}, V_N^*, S_{GV}^*)}$

$$\frac{\partial f_{(V_N, S_{GV}, V_N^*, S_{GV}^*)}}{\partial V_N} = {L_C}^H - [Z_B]\,{L_C}^{-1}\,\frac{\partial I_N}{\partial V_N}$$

$$\frac{\partial I_N}{\partial V_N} = \frac{\partial I_Y}{\partial V_N} + [YD]^T \frac{\partial I_\Delta}{\partial V_\Delta}[YD] - [Y_{sh}]$$

$$\frac{\partial I_Y}{\partial V_N} = \operatorname{diag}\left(-S_{LZY}^* - \frac{S_{LIY}^*}{2} \odot \frac{1}{|V_N|}\right)$$

$$\frac{\partial I_\Delta}{\partial V_\Delta} = \operatorname{diag}\left(-S_{LZ\Delta}^* - \frac{S_{LI\Delta}^*}{2} \odot \frac{1}{|V_\Delta|}\right)$$

$$\frac{\partial f_{(V_N, S_{GV}, V_N^*, S_{GV}^*)}}{\partial V_N^*} = -[Z_B]\,{L_C}^{-1}\,\frac{\partial I_N}{\partial V_N^*}$$

$$\frac{\partial I_N}{\partial V_N^*} = \frac{\partial I_Y}{\partial V_N^*} + [YD]^T \frac{\partial I_\Delta}{\partial V_\Delta^*}[YD]$$

$$\frac{\partial I_Y}{\partial V_N^*} = \operatorname{diag}\left(\frac{S_{LIY}^*}{2} \odot V_N^{0.5} \odot \frac{1}{V_N^{*1.5}} - (S_G^* - S_{LPY}^*) \odot \frac{1}{V_N^{*2}}\right)$$

$$\frac{\partial I_\Delta}{\partial V_\Delta^*} = \operatorname{diag}\left(\frac{S_{LI\Delta}^*}{2} \odot V_\Delta^{0.5} \odot \frac{1}{V_\Delta^{*1.5}} + S_{LP\Delta}^* \odot \frac{1}{V_\Delta^{*2}}\right)$$

$$\frac{\partial f_{(V_N, S_{GV}, V_N^*, S_{GV}^*)}}{\partial S_{GV}} = 0$$

$$\frac{\partial f_{(V_N, S_{GV}, V_N^*, S_{GV}^*)}}{\partial S_{GV}^*} = -\left[Z_B {L_C}^{-1}\right]_{GV} \operatorname{diag}\left(\frac{1}{V_{GV}^*}\right)$$

where $[\cdot]_{GV}$ and $\cdot_{GV}$ denote the columns and components related to generation nodes, respectively.

B. *Differentiation of* $f_{PV(V_N, S_{PV}, V_N^*, S_{PV}^*)}$

$$\frac{\partial f_{PV(V_N, S_{PV}, V_N^*, S_{PV}^*)}}{\partial V_{PV}} = \operatorname{diag}(V_{1PV}^*)\,[A_{PV}]$$

$$\frac{\partial f_{PV(V_N, S_{PV}, V_N^*, S_{PV}^*)}}{\partial V_{\sim PV}} = 0$$

$$\frac{\partial f_{PV(V_N, S_{PV}, V_N^*, S_{PV}^*)}}{\partial V_{PV}^*} = \operatorname{diag}(V_{1PV})\,[A_{PV}]^*$$

$$\frac{\partial f_{PV(V_N, S_{PV}, V_N^*, S_{PV}^*)}}{\partial V_{\sim PV}^*} = 0$$

$$\frac{\partial f_{PV(V_N, S_{PV}, V_N^*, S_{PV}^*)}}{\partial S_{PV}} = \frac{j}{2} I_{N_{PV} \times N_{PV}}$$

$$\frac{\partial f_{PV(V_N, S_{PV}, V_N^*, S_{PV}^*)}}{\partial S_{PV}^*} = \frac{j}{2} I_{N_{PV} \times N_{PV}}$$

where $V_{\sim PV}$ is the node voltages of all non-PV nodes.

C. *Differentiation of* $f_{VV(V_N, S_{VV}, V_N^*, S_{VV}^*)}$

$$\frac{\partial f_{\mathrm{VV}(\mathrm{V_N}, \mathrm{S_{VV}}, \mathrm{V_N^*}, \mathrm{S_{VV}^*})}}{\partial V_{VV}} = \frac{1}{2} \operatorname{diag}\left(N_k \odot V_{1VV}^{*\frac{1}{2}} \odot V_{1VV}^{-\frac{1}{2}}\right)[A_{VV}]$$

$$\frac{\partial f_{\mathrm{VV}(\mathrm{V_N}, \mathrm{S_{VV}}, \mathrm{V_N^*}, \mathrm{S_{VV}^*})}}{\partial V_{\sim VV}} = 0$$

$$\frac{\partial f_{\mathrm{VV}(\mathrm{V_N}, \mathrm{S_{VV}}, \mathrm{V_N^*}, \mathrm{S_{VV}^*})}}{\partial V_{VV}^*} = \frac{1}{2} \operatorname{diag}\left(N_k \odot V_{1VV}^{*-\frac{1}{2}} \odot V_{1VV}^{\frac{1}{2}}\right)[A_{VV}]^*$$

$$\frac{\partial f_{\mathrm{VV}(\mathrm{V_N}, \mathrm{S_{VV}}, \mathrm{V_N^*}, \mathrm{S_{VV}^*})}}{\partial V_{\sim VV}^*} = 0$$

$$\frac{\partial f_{VV(V_N, S_{VV}, V_N^*, S_{VV}^*)}}{\partial S_{VV}} = j I_{N_{VV} \times N_{VV}}$$

$$\frac{\partial f_{VV(V_N, S_{VV}, V_N^*, S_{VV}^*)}}{\partial S_{VV}^*} = 0$$

where $V_{\sim VV}$ is the node voltages of all non-VV nodes.

Appendix B

Expressing J^{-1} by submatrices Γ_A, Γ_B, Γ_C, and Γ_D, it's known that

$$\begin{bmatrix}\Gamma_A & \Gamma_B \\ \Gamma_C & \Gamma_D\end{bmatrix}\begin{bmatrix}j_A & j_B \\ j_B^* & j_A^*\end{bmatrix} = \begin{bmatrix}\mathrm{I} & 0 \\ 0 & \mathrm{I}\end{bmatrix}$$

By solving Γ_A and Γ_B, one obtains

$$\Gamma_A = (j_A - M\, j_B^*)^{-1}$$
$$\Gamma_B = -\Gamma_A\, M$$
$$M = j_B\, {j_A^*}^{-1}$$

And solving Γ_C and Γ_D

$$\Gamma_C = -\Gamma_D\, M^*$$
$$\Gamma_D = (j_A^* - M^*\, j_B)^{-1}$$

Note that $\Gamma_D = \Gamma_A^*$ and $\Gamma_C = \Gamma_B^*$.

This article has been accepted for publication in a future issue of this journal, but has not been fully edited. Content may change prior to final publication. Citation information: DOI 10.1109/TPWRS.2019.2892014, IEEE Transactions on Power Systems

APPENDIX C

The value Δz is obtained by solving

$$0 = J\begin{bmatrix}\Delta z \\ \Delta z^*\end{bmatrix} + \begin{bmatrix}h \\ h^*\end{bmatrix}$$

$$\Longrightarrow \begin{bmatrix}\Delta z \\ \Delta z^*\end{bmatrix} = -J^{-1}\begin{bmatrix}h \\ h^*\end{bmatrix}$$

$$\begin{bmatrix}\Delta z \\ \Delta z^*\end{bmatrix} = -\begin{bmatrix}\Gamma_A & -\Gamma_A M \\ -\Gamma_A^* M^* & \Gamma_A^*\end{bmatrix}\begin{bmatrix}h \\ h^*\end{bmatrix}$$

$$\Delta z = \Gamma_A(Mh^* - h)$$

APPENDIX D

It is considered that the transformer ratio T provides the secondary voltages by left-multiplying T to the primary voltages. The following Table shows T for five usual connections in distribution networks.

TRANSFORMER RATIO VS. CONNECTIONS

1^{ry} \ 2^{ry}	Delta	Open Delta	Grounded Wye
Delta	$W\ T_W[YD]$	-----	$T_W[YD]$
Ungrounded Wye	$W\ T_W\ U$	-----	-----
Grounded Wye	-----	-----	T_W
Open Wye	-----	$W\ O_\Delta\ T_W\ O_Y$	-----

The matrix W provides the equivalent phase voltages as a function of line-to-line voltages [23]:

$$W = \frac{1}{3}\begin{bmatrix}2 & 1 & \\ & 2 & 1 \\ 1 & & 2\end{bmatrix}$$

The matrix U obtains line-to-neutral voltages from known phase voltages, for Ungrounded Wye connections. U overrides the zero sequence-component of three phasors:

$$U = \begin{bmatrix}1 & 1 & 1 \\ 1 & a^2 & a \\ 1 & a & a^2\end{bmatrix}\frac{1}{3}\begin{bmatrix}0 & 0 & 0 \\ 1 & a & a^2 \\ 1 & a^2 & a\end{bmatrix} = \frac{1}{3}\begin{bmatrix}2 & -1 & -1 \\ -1 & 2 & -1 \\ -1 & -1 & 2\end{bmatrix}$$

In Open Wye-Open Delta connections when phase p is open, $O_{Y,p}$ obtains two line-to-neutral voltages from two known phase voltages on the Wye side. $O_{Y,p}$ overrides the zero sequence-component of two phasors (its size is 3x3 for convenience). The matrix $O_{\Delta,p}$ obtains three line-to-line voltages from two known line-to-line voltages on the Delta side:

$$O_{Y,1} = \frac{1}{2}\begin{bmatrix}0 & & \\ & 1 & -1 \\ & -1 & 1\end{bmatrix} \qquad O_{\Delta,1} = \begin{bmatrix}0 & -1 & -1 \\ & 1 & \\ & & 1\end{bmatrix}$$

$$O_{Y,2} = \frac{1}{2}\begin{bmatrix}1 & & -1 \\ & 0 & \\ -1 & & 1\end{bmatrix} \qquad O_{\Delta,2} = \begin{bmatrix}1 & & \\ -1 & 0 & -1 \\ & & 1\end{bmatrix}$$

$$O_{Y,3} = \frac{1}{2}\begin{bmatrix}1 & -1 & \\ -1 & 1 & \\ & & 0\end{bmatrix} \qquad O_{\Delta,3} = \begin{bmatrix}1 & & \\ & 1 & \\ -1 & -1 & 0\end{bmatrix}$$

T_W is the matrix of turns ratio. For a three-phase transformer bank integrated by three single-phase transformers with turns ratios t_1, t_2 ,and t_3, the $T_W = \mathrm{diag}([t_1 \quad t_2 \quad t_3])$

ACKNOWLEDGMENT

The authors thank CAPES (Brazilian research agency) for supporting this work.

REFERENCES

[1] V. Ajjarapu and C. Christy, "The continuation power flow: A tool for steady state voltage stability analysis," *IEEE Trans. Power Syst.*, vol. 7, no. 1, pp. 416–423, 1992.
[2] F. W. Mohn and A. C. Zambroni de Souza, "Tracing PV and QV curves with the help of a CRIC continuation method," *IEEE Trans. Power Syst.*, vol. 21, no. 3, pp. 1115–1122, 2006.
[3] A. Gómez-Expósito, A. J. Conejo, and C. A. Cañizares, *Electric Energy Systems: Analysis and Operation*, 2nd Ed. Boca Raton, Florida: CRC Press, 2018.
[4] C. S. Cheng and D. Shirmohammadi, "A Three-phase Power Flow Method For Real-Time Distribution System Analysis," *IEEE Trans. Power Syst.*, vol. 10, no. 2, pp. 671–679, 1995.
[5] E. Bompard, E. Carpaneto, G. Chicco, and R. Napoli, "Convergence of the backward/forward sweep method for the load-flow analysis of radial distribution systems," *Int. J. Electr. Power Energy Syst.*, vol. 22, no. 7, pp. 521–530, 2000.
[6] L. Ramos de Araujo, D. R. Ribeiro Penido, N. Alves do Amaral Filho, and T. A. Pereira Beneteli, "Sensitivity analysis of convergence characteristics in power flow methods for distribution systems," *Int. J. Electr. Power Energy Syst.*, vol. 97, pp. 211–219, 2018.
[7] S. K. Goswami and S. K. Basu, "Direct solution of distribution systems," *IEE Proc. C - Gener. Transm. Distrib.*, vol. 138, no. 1, pp. 78–88, 1991.
[8] J.-H. Teng, "A direct approach for distribution system load flow solutions," *IEEE Trans. Power Deliv.*, vol. 18, no. 3, pp. 882–887, 2003.
[9] U. Ghatak and V. Mukherjee, "A fast and efficient load flow technique for unbalanced distribution system," *Int. J. Electr. Power Energy Syst.*, vol. 84, pp. 99–110, 2017.
[10] G. W. Chang, S. Y. Chu, and H. L. Wang, "An improved backward/forward sweep load flow algorithm for radial distribution systems," *IEEE Trans. Power Syst.*, vol. 22, no. 2, pp. 882–884, 2007.
[11] U. Ghatak and V. Mukherjee, "An improved load flow technique based on load current injection for modern distribution system," *Int. J. Electr. Power Energy Syst.*, vol. 84, pp. 168–181, 2017.
[12] T. Alinjak, I. Pavić, and M. Stojkov, "Improvement of backward/forward sweep power flow method by using modified breadth-first search strategy," *IET Gener. Transm. Distrib.*, vol. 11, no. 1, pp. 102–109, 2017.
[13] A. Garces, "A Linear Three-Phase Load Flow for Power Distribution Systems," *IEEE Trans. Power Syst.*, vol. 31, no. 1, pp. 827–828, 2016.
[14] T. T. Nguyen and C. T. Vu, "Complex-variable Newton-Raphson load-flow analysis with FACTS devices," in *IEEE PES Transmission and Distribution Conference and Exhibition*, 2006.
[15] Z. Wang, B. Cui, and J. Wang, "A Necessary Condition for Power Flow Insolvability in Power Distribution Systems with Distributed Generators," *IEEE Trans. Power Syst.*, vol. 32, no. 2, pp. 1440–1450, 2017.
[16] R. Pires, "Complex-Valued Steady-State Models as Applied to Power Flow Analysis and Power System State Estimation," Ph.D. dissertation, Federal University of Itajubá, 2017.
[17] I. Džafić, R. A. Jabr, and T. Hrnjić, "High Performance Distribution Network Power Flow using Wirtinger Calculus," *IEEE Transactions on Smart on Smart Grid*, 2018.
[18] J. E. Sarmiento, E. M. Carreno, and A. C. Zambroni de Souza, "Modeling inverters with volt-var functions in grid-connected mode and droop control method in islanded mode," *Electr. Power Syst. Res.*, vol. 155, pp. 265–273, 2018.
[19] W. Wirtinger, "Zur formalen Theorie der Funktionen von mehr komplexen Veränderlichen," *Math. Ann.*, vol. 97, pp. 357–376, 1927.
[20] K. Kreutz-Delgado, "The Complex Gradient Operator and the CR-Calculus." San Diego, 2009.
[21] P. Bouboulis, "Wirtinger's Calculus in general Hilbert Spaces." 2010.
[22] IEEE PES AMPS DSAS Test Feeder Working group, "Test Feeders." [Online]. Available: http://sites.ieee.org/pes-testfeeders/resources/. [Accessed: 08-May-2018].
[23] W. H. Kersting, *Distribution System Modeling and Analysis*, 3rd ed. Las Cruces, New Mexico: CRC Press, 2012.